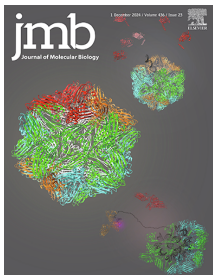

Unraveling the Membrane Topology of TMEM151A: A Step Towards Understanding its Cellular Role

Lisastella Morinelli [1,2,†], Beatrice Corradi [1,2,†], Pietro Arnaldi [1], Katia Cortese [1,3], Martina Muià [1], Federico Zara [5,6], Luca Maragliano [2,4], Bruno Sterlini [1,3,‡], and Anna Corradi [1,3,‡,*]

*1 - **University of Genova,** Department of Experimental Medicine, Genova, Italy*
*2 - **Istituto Italiano di Tecnologia,** Center for Synaptic Neuroscience and Technology, Genova, Italy*
*3 - **IRCCS Ospedale Policlinico San Martino,** Genova, Italy*
*4 - **Polytechnic University of Marche,** Department of Life and Environmental Sciences, Ancona, Italy*
*5 - **University of Genova,** Department of Neurosciences, Rehabilitation, Ophthalmology, Genetics, Maternal and Child Health, Genova, Italy*
*6 - **IRCCS Istituto Giannina Gaslini,** Unit of Medical Genetics, Genova, Italy*

***Correspondence to Anna Corradi:** anna.corradi@unige.it (A. Corradi)*
https://doi.org/10.1016/j.jmb.2024.168834
Edited by Lutz Schmitt

Abstract

Transmembrane protein 151A (TMEM151A) has been identified as a causative gene for paroxysmal kinesigenic dyskinesia, though its molecular function remains almost completely unknown. Understanding the membrane topology of transmembrane proteins is crucial for elucidating their functions and possible interacting partners. In this study, we utilized molecular dynamics simulations, immunocytochemistry, and electron microscopy to define the topology of TMEM151A. Our results validate a starting AlphaFold model of TMEM151A and reveal that it comprises a transmembrane domain with two membrane-spanning alpha helices connected by a short extracellular loop and an intramembrane helix-hinge-helix structure. Notably, most of the protein is oriented towards the intracellular side of the membranes with a large cytosolic domain featuring a combination of alpha-helix and beta-sheet structures, as well as the protein N- and C-termini. These insights into TMEM151A's topology and orientation of its domains with respect of the cell membranes provide essential information for future functional studies and represent a first fundamental step for understanding its role in the pathogenesis of paroxysmal kinesigenic dyskinesia.

Introduction

The Transmembrane protein 151A (*TMEM151A*) has been recently identified as a causative gene for the Paroxysmal Kinesigenic Dyskinesia (PKD).[1–11] This rare autosomal dominant movement disorder, occurring in adolescence and typically characterized by recurrent involuntary movements attacks, was previously associated mostly to the Proline Rich Transmembrane protein 2 (*PRRT2*) mutations.[12,13] *PRRT2* encodes for a protein that controls neuronal excitability and network stability by negatively modulating the function of Voltage Gated Sodium channels and regulating synaptic activity.[14–19]

TMEM151A is an almost uncharacterized gene consisting of two exons encoding a 468-amino acid protein. In mice, *Tmem151A* mRNA is expressed at the level of the nervous system in the cortex, hippocampus, brainstem and spinal

cord. Interestingly, the expression is higher in postnatal stages and decreases in adulthood as the symptoms of the disease that appear in late childhood or in adolescence and then disappear in most cases in adulthood. There are no protein expression data except for overexpression experiments suggesting a higher association of TMEM151A with endoplasmic reticulum membranes (ER).[1]

Interestingly, the drug treatment of choice for PKD caused by TMEM151A or PRRT2 mutations is Carbamazepine, a sodium channel blocker.[1–11] This evidence, together with the similar expression pattern in the central nervous system and that both are transmembrane proteins, may suggest similar pathophysiological functions.

TMEM151A is part of the TMEM proteins, a large family of poorly described membrane proteins containing at least one putative transmembrane segment that spans completely or partially biological membranes.[20]

Depending on their membrane topology and domains' orientation, TMEM proteins are involved in extracellular functions such as cell–cell communication and adhesion processes or in intracellular functions like mechanisms of exo or endocytosis. In the neuronal setting, cell membrane proteins with large extracellular domains may be involved in the neuronal/glial interactions or in synapse formation and functioning. Otherwise, cell membrane proteins with large intracellular domains, like PRRT2, may interact and regulate other membrane proteins, like channels, or be involved in membrane trafficking mechanisms or in neurotransmitter release.[14,21,22] Therefore, the different orientation of protein domains as well as the NH2 and COOH termini of a protein with respect to the cell membrane may determine a completely diverse set of putative protein interactors, and the formulation of different hypotheses about their function.

TMEM151A is predicted to have two transmembrane helices connected by an extramembranous loop, followed by a quite large extramembranous domain. The orientation of the NH2 and COOH termini is unknown and as a consequence its membrane topology and the location of the protein domains with respect to cell membranes is still unclear.

The definition of the topology of TMEM151A, and therefore of the orientation of the large extramembranous domain, may represent a first fundamental step forward in the understanding of TMEM151A function at the membrane level.

Here, we show the membrane topology of TMEM151A. We started from AlphaFold structural prediction and we refined it by molecular dynamics (MD) simulations and by two different experimental approaches: the live-labeling immunofluorescence (IF) and the immunogold electron microscopy. The understanding of TMEM151A topology is crucial to understand the essential features of the protein and its pathophysiological role. Although some aspects of the PRRT2 function have been clarified, the pathophysiological mechanisms of PKD remain unclear, therefore complementing hints coming from the investigation of TMEM151A may contribute to shed light on this disorder.

Materials and Methods

Structural modeling

The predicted structure of full-length TMEM151A was retrieved from the AlphaFold2 (AF2) database.[23] Amino-acids M1 to P21 and S323 to L468, characterized by low values of the AF2 confidence metrics (the predicted local distance difference test score, pLDDT) were removed. All the retained protein segments show optimal values of pLDDT, except for a two-turns helix in the short extramembranous loop. The resulting model was submitted to the Orientations of Proteins in Membranes[24] (OPM-PPM) web server to predict its orientation within a membrane-like environment. PyMOL[25] was used for visual inspection and image generation.

All-atom molecular dynamics simulations of truncated TMEM151A

The membrane builder plug-in of the CHARMM-GUI[26] web server was utilized for setting up the system and for generating input file to be used in MD simulations. The protein model (residues L22 to S322) was inserted into a 1-palmitoyl-2-oleoyl-*sn*-glycero-3-phosphocholine (POPC) lipid bilayer and solvated with TIP3P water molecules in a [170.09 $\times$ 170.09 $\times$ 159.03] $Å^3$ rectangular box.[27] Na^+ and Cl^- ions were added to neutralize the total system's charge at a concentration of 0.15 M. The whole system amounts to $\sim$435000 atoms.

Simulations were performed with namd2.14[28] using the CHARMM36m force field.[29,30] Periodic boundary conditions (PBC) were applied. Electrostatic interactions were treated with the Particle Mesh Ewald method,[31] with a maximum grid spacing of 1 Å and an interpolation order of 6. A cut-off of 12 Å was employed for Lennard-Jones interactions, which were smoothly switched off starting at 10 Å. Chemical bond distances involving hydrogen atoms were constrained using the SHAKE/RATTLE algorithm.[32] A time-step of 2 fs was employed.

Before production stage, the system was energy minimized and equilibrated for 40 ns in the isobaric-isothermal ensemble (NPT), extending the protocol suggested by CHARMM-GUI, with P = 1 atm and T = 310 K. Pressure and temperature were maintained constant using the Nosé-Hoover Langevin piston[33] and the Langevin thermostat, respectively. Afterwards, three inde-

pendent, 500-ns-long unbiased all-atom MD simulations were performed in the NPT ensemble.

Structural analysis

The VMD software[34] and TcL scripting were used to compute root mean square deviations (RMSDs) for the transmembrane (TMD) and the extramembrane domains. The integrity of TMD's helices spatial arrangement was monitored by computing cross-distances between Cα atoms.

The TrajMap[35] program was utilized to calculate each residue's backbone shift (defined as the Euclidean distance after alignment) from the starting position of the simulation. To this goal, each of the three trajectories was filtered by extracting two configurations per 10 ns. Derived structures were aligned to eliminate rotations and translations.

A structural alignment between AF3[36] and AF2 models of human TMEM151A was performed.

Multiple sequence alignment

Human TMEM151A full-length sequence served as a query for a homology search which was carried out using the NCBI-blastp[37] (protein–protein BLAST) algorithm. The Reference proteins (refseq_protein) database was scanned while excluding models; the maximum number of aligned hits was set to 50, while the expect threshold was set to 0.005 with a word size of 5. The BLOSUM62 scoring matrix was chosen and penalties for the insertion and extension of a gap were set to 11 and 1, respectively. Eleven sequences were retrieved which were subsequently aligned with M-Coffee.[38,39] The multiple sequence alignment file was later visualized and edited using Espript3.0.[40] A similarity score for each column of the MSA was calculated considering the percentage of strictly conserved residues. The results of the conservation analysis were converted in a structural map.

Constructs

We generated four distinct HA constructs using the pKH3 plasmid (pKH3 was a gift from Ian Macara, Addgene plasmid #12555; https://n2t.net/addgene:12555; RRID:Addgene_12555)[41]: 3xHA tags at the N terminus of TMEM151A (HA-TMEM151A), with the TMEM151A human coding sequence cloned in EcoR1 site; 3xHA tags at the C terminus of TMEM151A (TMEM151A-HA), with the TMEM151A human coding sequence without a stop codon cloned in HindIII-SalI; 2xHA tags between the two hydrophobic transmembrane segments in the putative extramembranous loop of the protein (TMEM151A-HA-LOOP), obtained by cloning *TMEM151A* in HindIII-EcoRI and then by cloning 2xHA tags in XmaI site in the *TMEM151A* sequence; 2xHA tags between the two β-sheet forming segments (TMEM151A-HA-βsheet), obtained by cloning *TMEM151A* in HindIII-EcoRI and then, by cloning into PstI-XhoI, we inserted a modified sequence with 2xHA tags after Asparagine 170 (generated by Genscript Synthesis Service).

For the double tagged TMEM151A-HA-LOOP + V5 construct, the TMEM151A-HA-LOOP construct was modified with the addition of a V5 tag at the C terminus after the removal of the stop codon by cloning the V5 tag in XbaI-EcoRI sites (top oligo 5′-[PHO] CTA GAG GTA AGC CTA TCC CTA ACC CTC TCC TCG GTC TCG ATT CTA CGT AGG; bottom oligo 5′-[PHO] AAT TCC TAC GTA GAA TCG AGA CCG AGG AGA GGG TTA GGG ATA GGC TTA CCT).

All primers and oligos were purchased from Eurofins Genomics (Kholn, Germany).

Cell culture and transfection

HEK293 cell lines were maintained in DMEM/F12 (1:1) supplemented with 10% fetal bovine serum, 100 U/ml penicillin and 100 μg/ml streptomycin. Cell lines were transfected according to the manufacturer's recommendations at 70% confluency using Lipofectamine 2000. All reagents were purchased from ThermoFisher Scientific.

Immunolabeling

HEK293 cells transfected with TMEM151A-HA, HA-TMEM151A, TMEM151A-HA-LOOP or TMEM151A-HA-βsheet constructs were live-labeled as schematized in Figure S4.

In the live-labeling protocol, the cells are incubated with the primary antibody diluted in the culture medium; without the permeabilization step, the primary antibodies can bind just to epitopes exposed on the extracellular side of the cell membrane. Transfected HEK293 cells were maintained for 10 min at 4 °C, and then were live labeled by incubation with primary anti-HA mouse antibody (Cat.#05-904; Merck Millipore, 1:200 diluted in culture medium) for 20 min at 4 °C to detect surface epitopes. Samples were washed in PBS and then incubated with the Alexa Fluor 488-conjugated secondary antibody (Invitrogen, 1:500 diluted in culture medium) for 20 min at 4 °C and then were fixed by 4% paraformaldehyde (PFA) for 20 min at room temperature (RT). After washes in PBS, we performed a standard IF staining: cells were permeabilized with 0.1% Triton X-100 in PBS for 10 min at RT, and after washes, blocking was performed with 3% bovine serum albumin (BSA) for 45 min at RT. Samples were then incubated with anti-TMEM151A rabbit antibody (Cat.#HPA041035, immunogenic sequence: EVPALIPDGEPLREEQRPLKQSLGSSLC; Sigma Aldrich, 1:500 diluted in 3% BSA), washed in PBS, and incubated with Alexa Fluor 594-conjugated secondary antibody (Invitrogen; 1:500 in 3% BSA). After several washes in PBS, coverslips were mounted using Prolong Gold

antifade reagent (Invitrogen) containing 4′,6′-diamidino-2-phenylindole (DAPI) for nuclear staining. For the TMEM151A-HA-LOOP + V5 construct experiments, the primary anti-HA mouse antibody (Cat.#05-904; Merck Millipore) and the primary anti-V5 rabbit antibody (Cat.#13202; Cell Signaling Technology) were used, in different combinations of live-labeling and standard IF.

SDS-PAGE and Western blotting

For sodium dodecylsulfate gel electrophoresis (SDS-PAGE), samples heated to 98 °C for 5 min without boiling were run on 10% (w/v) polyacrylamide gels and blotted onto nitrocellulose membranes (Whatman). Blotted membranes were blocked for 1 h in 5% milk in Tris-buffered saline (10 mM Tris, 150 mM NaCl, pH 8.0) plus 0.1% Triton X-100 and incubated overnight at 4 °C with the appropriate primary antibody. Membranes were washed and incubated at room temperature for 1 h with peroxidase-conjugated anti-mouse (1:3000; BioRad, Hercules, CA) or anti-rabbit (1:3000; BioRad, Hercules, CA) antibodies. Bands were revealed with the ECL chemiluminescence detection system (ThermoFisher Scientific). Immunoblots were quantified by densitometric analysis of the fluorograms (Quantity One software; Bio-Rad, Hercules, CA) obtained in the linear range of the emulsion response.

Pre-embedding immunogold labeling for electron microscopy

HEK293 cells were plated in 2 well permanox-coated plates (Nunc, LabTek Chamber Slides, 177372) and transfected with TMEM151A-HA or TMEM151A-HA-LOOP constructs. After 24 h, cells were rinsed in PBS and fixed with 3% paraformaldehyde + 0.05% glutaraldehyde in PBS for 1 h at RT. For immunolabeling, the cells were briefly washed in PBS, permeabilized in blocking solution (50 mM NH 4 Cl, 0.5% BSA, 0.1% saponin in PBS) for 30 min and incubated overnight with primary anti-HA rabbit antibody (Cat.#71-5500; ThermoFisherScientific, 1:100 diluted in blocking solution), then rinsed and incubated with 5-nm gold-labeled protein A (PAG-5 nm, purchased from Utrecht University, Utrecht, The Netherlands) for 4 h at RT. After washes, cells were fixed in 2.5% glutaraldehyde in 0.1 M sodium cacodylate for 1 h at RT and postfixed in 2% OsO_4 in water for 1 h at RT, contrasted *en bloc* with 1% uranyl acetate for 1 h, dehydrated in a graded series of ethanol, and embedded in Epoxy resin for 2 days at 60 °C. 50 nm ultrathin sections were cut by Leica Ultracut UCT ultramicrotome and further contrasted with lead citrate and 5% uranyl acetate in ethanol.[42] Ultrathin sections were examined with an HT7800 120Kv transmission electron microscope (Hitachi, Tokyo, Japan) equipped with Megaview G3 camera and Radius 2.0 software (EMSIS, Muenster, Germany).

Results

Structural modeling of TMEM151A

We retrieved the AlphaFold2 (AF2) predicted model of full-length TMEM151A (Figure S1A). The model displays a short unstructured N-terminal segment, an all-α-helix domain, a mixed α-helix/β-sheet domain and a long mostly unstructured C-terminal region. The domain comprised between residues L22 to S322 has the highest degree of model confidence, as shown by the AF2 per-residue confidence estimation (pLDDT), whose values are mostly larger than 90 over 100 in this region (Figure S1A, B). A prediction performed by AF3 showed pLDDT values similar to AF2 in all domains, and an almost identical three-dimensional fold of the high-confidence segment (L22 to S322, Figure S1B).

Multiple sequence alignment

We performed a homology search in the Reference proteins database using the full-length sequence of human TMEM151A as query; eleven hits were retrieved pertaining to different eukaryotes. The multiple sequence alignment (MSA) total score was 853 and the best alignment outcomes were reached for bull TMEM151B1 (93 points), rat TMEM151A (93 points) and mouse TMEM151A (92 points) sequences.

On a total of 617 alignment columns, 109 (17.67%) display strict conservation, 78 (12.64%) show conservative substitutions, 42 (6.81%) highlight semi-conservative substitutions while the other 388 columns (62,88%) are non-conserved (Figure S1D). We grouped identically conserved positions with those that are conservatively substituted, and we refer to them simply as conserved. By mapping the MSA results on the protein structure, we can observe that conserved residues mainly localize in folded secondary structure elements, without a specific preference for α-helix or β-sheet traits (Figure S1C).

All-atom molecular dynamics simulations of truncated TMEM151A

We used MD simulations to refine and assess the TMEM151A AF2 structural model, considering only the high-confidence segment from L22 to S322 (Figure S1B). The OPM-PPM web server yielded the predicted position of the protein embedded in a membrane, and a free-energy difference of transfer from water to the membrane of −28.3 kcal/mol,[24] a value that characterizes integral membrane proteins. The protein was then inserted in a POPC membrane and solvated with water and ions. The whole system was energy-

minimized and equilibrated with MD by extending the CHARMM-GUI standard protocol. The conformation of the protein within the membrane at the end of the equilibration stage is shown in Figure 1. Based on this structure, we identified the following motifs. A transmembrane domain (TMD), comprising two membrane-spanning alpha helices, H1 (residues L33-L64) and H2 (Y98-Q126), and a helix-hinge-helix motif with the short helices H5 (A285-A294) and H6 (L296 to G307), located further on the protein sequence. H1 and H2 helices are connected by an extramembrane loop (V67-A91) including a short helix (extramembrane domain 1, EM1), while on the other side of the membrane is a much larger soluble domain, formed by residues A127 to R284 and T308 to S322 (extramembrane domain 2, EM2). The EM2 includes two antiparallel beta-sheets, β1 and β2, each of which contacts an α-helix (H3, formed by A132-Q144, and H4, by A229-N246). β1 is formed by strands S1-S2 (P147-R169 and D172-E192) and S4 (Y252-L261), with the first two extending into a long β-hairpin motif. β2 includes strands S3, S5 and S6, identified by residues A215-F226, S269-F273 and A309-F319, respectively. In the conformation at the end of the equilibration, the tip of the β-hairpin interacts with the membrane's leaflet via the linker between strands S1 and S2 (residues R167-A173).

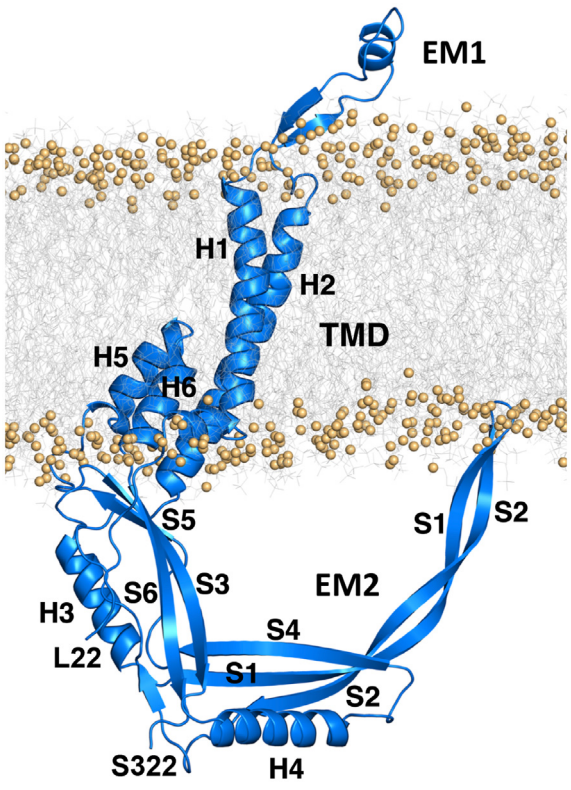

Figure 1. Truncated TMEM151A structure in the lipid membrane after MD equilibration. The TMEM151A domain from L22 to S322 of TMEM151A is represented as blue cartoon; phospholipids heads as yellow spheres and tails as gray sticks. Water molecules are not shown for clarity. The different structural motifs are indicated. EM1: extramembrane domain 1, TMD: transmembrane domain, EM2: extramembrane domain 2, H: alpha-helix, S: β-strands.

After equilibration, three independent 500-ns long simulations were performed. In all trajectories, the overall three-dimensional structure of the protein was conserved, as revealed by backbone root-mean-square deviation (RMSD) (Figure 2A). In particular, very limited structural fluctuations were observed for the TMD, whose stability was additionally confirmed by the time-evolution of inter-helices cross-distances (Figure S2), while the EM2 showed larger fluctuations. Indeed, along the simulations we observed different conformations for the long β-hairpin, in which its tip is associated to the membrane, near to, or, only occasionally, quite far from it (completely dissociated). To monitor this heterogeneity, we computed the time-evolution of the distance between the center of mass (COM) of residues R167-A173 and the COM of leaflet's phosphorous atoms (Figure 2B). Snapshots illustrating distinct characteristic conformations are reported in Figure 2C.

The per-residue contribution to protein conformational fluctuations was assessed by calculating each residue's Euclidean distance (defined *shift*) from the starting position of the simulation after structural alignment (Figures 3A, B and S3). In all the three replicas, the β-hairpin motif and the EM1 appear as the most mobile segments.

Live-labeling immunofluorescence defines the orientation of TMEM151A in the membrane

To determine the orientation of the EM1 and EM2 domains resulting from the in-silico simulations, we generated four distinct constructs (schematized in Figure 4A) bearing a triplet or duplet of HA tags alternatively at the N terminus (HA-TMEM151A), at the C terminus (TMEM151A-HA), within the loop (EM1) connecting the two transmembrane helices H1 and H2 (TMEM151A-HA-LOOP) or in the β1 structure at the level of the β-hairpin tip connecting the two β-strands S1-S2 (TMEM151A-HA-βsheet). AF2 generated models of the constructs show that the inserted tags do not alter the secondary or tertiary structure of truncated TMEM151A (Figure S4). While the pLDDT scores of the tag segments were very low, those of the protein were the same as the original model.

We transfected HEK293 cells with the four constructs and performed a live-labeling IF with anti-HA antibody followed by permeabilization and standard IF with anti-TMEM151A antibody (targeting an intracellular epitope, see Figure S5B, C for antibody specificity) as schematized in Figure S5A. During the live-labeling protocol cells

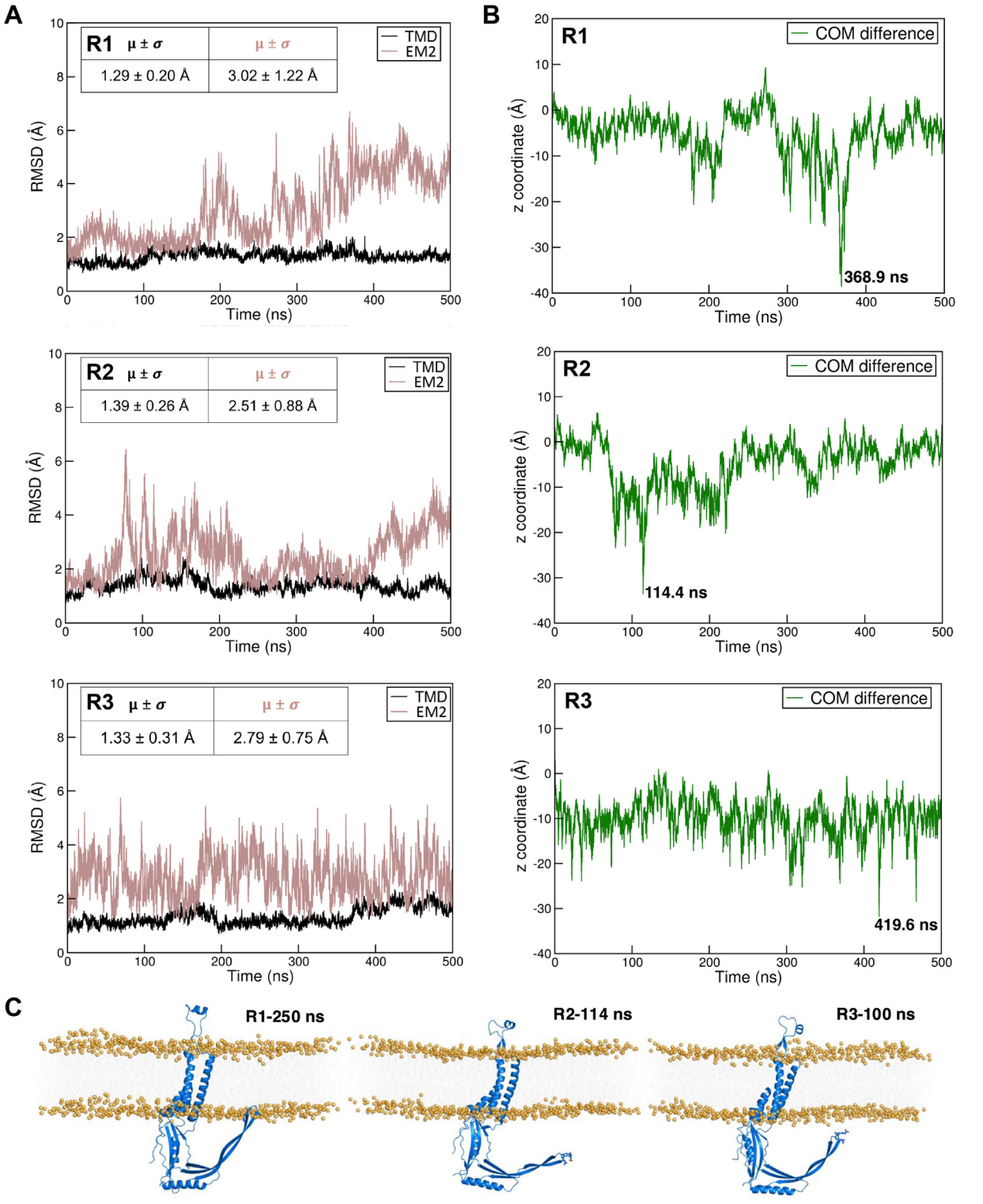

Figure 2. Molecular dynamics simulations of TMEM151A. A. Time evolution of backbone RMSD for truncated TMEM151A in the three replicated trajectories (R1-R3), for the α transmembrane domain (TMD, black), and the extramembrane domain 2 (EM2, brown). For each profile, average (μ) and Standard deviation (σ) values are reported. B. Time evolution of the distance along the z axis between the COM of R167-A173 α carbons and the COM of the phosphorus atoms in the lower leaflet. Frames corresponding to peak values are labelled. C. Snapshots extracted from the three MD trajectories at selected time-frames.

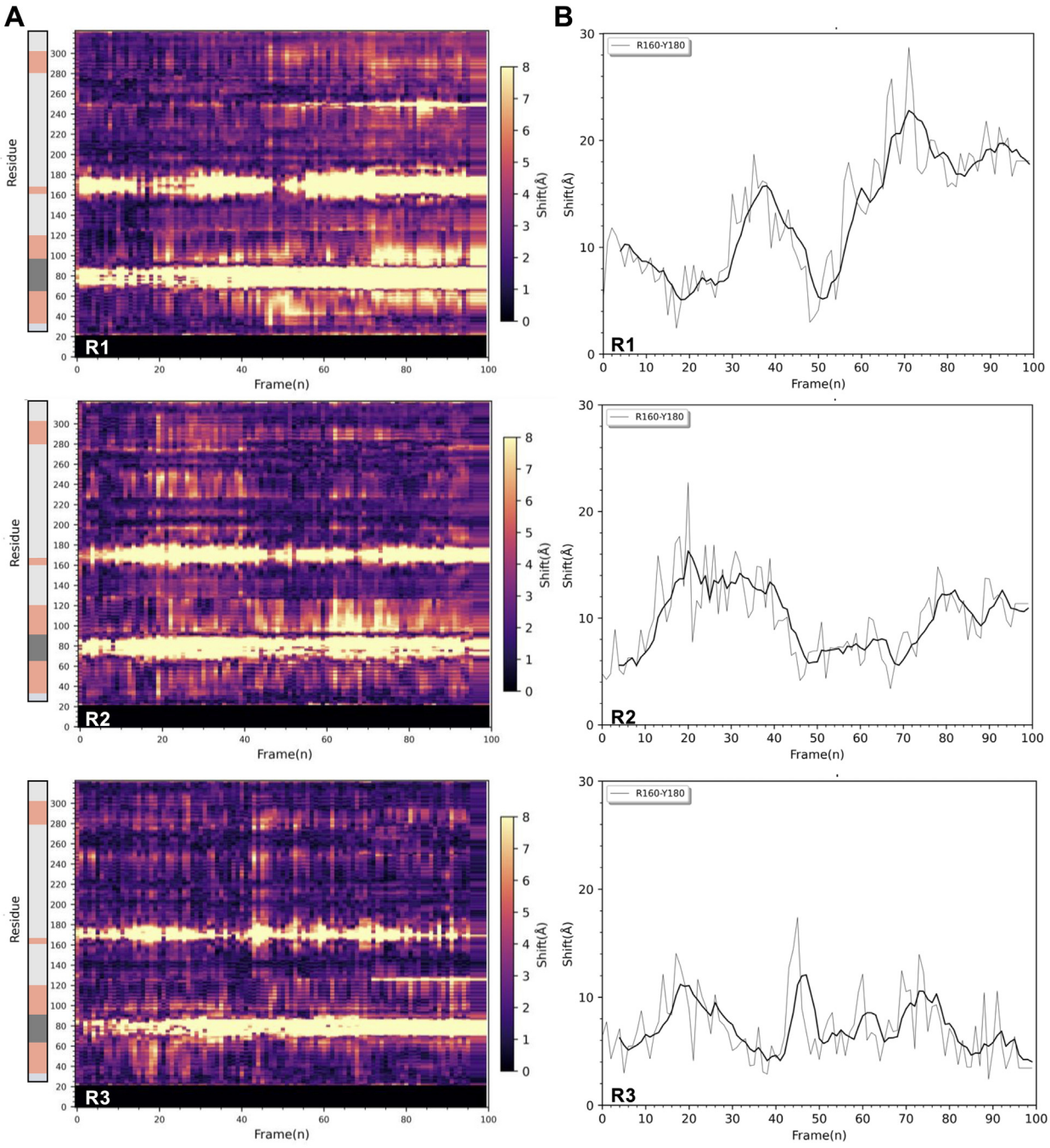

Figure 3. Protein's atomic fluctuations. A. Time evolution of each residue's backbone shift (the Euclidean distance after alignment) from the starting position in the three trajectories, colored according to their amplitude following the color bar on the right. The color bar on the left indicates the localization of each residue (numbers on the y-axis) according to the code: light grey for EM2, pink for transmembrane and dark grey for EM1. B. Time evolution of residue's backbone shift for TMEM151A β-hairpin (R160-Y180). Thick black lines represent moving average computed with a stride of 5 frames for each replica.

preserve the cell membrane integrity, therefore, only the HA-epitopes which are exposed extracellularly can be recognized by the antibody. In these conditions, HA antibodies exclusively recognized the TMEM151A-HA-LOOP isoform expressing cells, confirming exposure of this loop to the extracellular surface (Figure 4B, upper lane), whereas no signal could be detected in live cells transfected with the other constructs, confirming that the N and C termini, as well as the β-hairpin tip loop, are located intracellularly. After permeabilization, we performed standard IF with

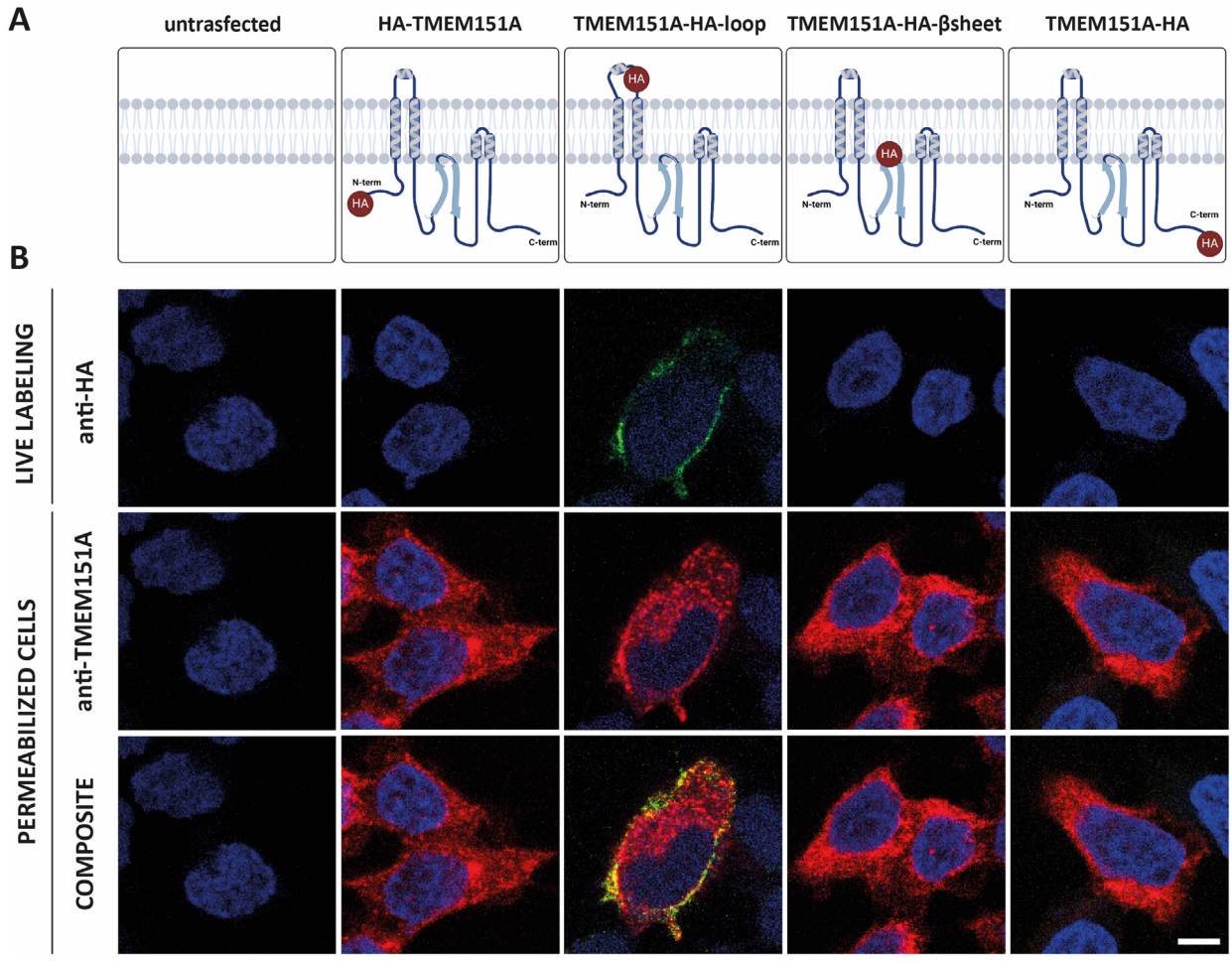

Figure 4. Live-labeling immunofluorescence defines the orientation of TMEM151A in the membrane. A. Schematic representation of HEK293 cells untransfected or transfected with different TMEM151A constructs, showing the HA tags positioning in the predicted TMEM151A membrane topology. B. Representative confocal images of HEK293 cells untransfected or transfected with either HA-TMEM151A, TMEM151A-HA-LOOP, TMEM151A-HA-βsheet or TMEM151A-HA, live-labeled with anti-HA antibody (upper panel, green) and labeled with anti-TMEM151A (middle panel, red). Merged images (bottom panel). Scale bar 5 μm.

anti-TMEM151A antibody, aimed to visualize the total TMEM151A expression and that the cells negative for live labeling are actually transfected. After this step, all four TMEM151A isoforms were detected with comparable expression levels (Figure 4B, middle lane).

To have a further validation of the described membrane topology, we generated a double tagged TMEM151A construct presenting a duplet of HA tag in the EM1 loop and a V5 tag at the C terminus of the protein (Figure S6). Live-labeling IF using anti-HA antibody resulted in a positive membrane staining, while no signal was present by anti-V5 antibody labeling. In the standard IF performed afterwards, the permeabilization led both anti-HA and anti-V5 antibodies to give positive cellular signals (Figure S6). Therefore, only the combination of the anti-HA live labeling signal (in green) with the anti-V5 permeabilized signal (in red) resulted in a merged signal (yellow) at the membrane level. These results demonstrate that EM1 connecting H1 and H2 helices is extracellular whereas the large soluble EM2 domain is oriented towards the cytosol, as schematized in Figure 4A.

Electron microscopy confirms TMEM151A membrane topology

To analyze the TMEM151A topology in a greater detail, we transfected HEK293 cells with TMEM151A-HA-LOOP and TMEM151A-HA constructs, that expose HA epitopes on the opposite sides of the membrane (see Figure 4), and performed immunogold labeling followed by electron microscopy analysis. As expected, cells transfected with TMEM151A-HA-LOOP showed the gold particles localized outside of the plasma

membrane (Figure 5A, upper images) and, although more rarely, in the internal part of putative endosomes (Figure 5A, bottom images). On the contrary, in the cells transfected with the TMEM151A-HA, gold particles are visualized at the internal side of the plasma membrane (Figure 5B, upper image) and more frequently at the cytosolic face of the ER (Figure 5B, lower images) and of the endosomes (Figure 5B, upper images). These results confirm an opposite localization of the HA epitopes of the TMEM151A-HA-LOOP and the TMEM151A-HA constructs with respect to the cellular membranes and further confirm the predicted topology. In addition, taken together, our confocal and electron microscopy data support the results by Li et al. regarding the presence of TMEM151A overexpressed protein at the level of intracellular membranes, in particular of the ER and endosomal structures, as well as provide new information about its localization at the plasma membrane.[1]

Discussion

TMEM151A is a virtually unknown protein that has recently been associated with PKD, a movement disorder causing frequent dyskinesial attacks, highly impacting the quality of life of patients, mostly children or adolescents. It is therefore of pivotal importance to understand the function of TMEM151A in order to improve therapies.

As a first step to understand its biological function, we identified the topology of TMEM151A by a combination of computational and experimental approaches. Structural modeling and refinement by MD identified well-separated transmembrane and extramembrane domains. TMD encompasses two major helices (H1 and H2) that span the whole membrane and are connected by a short loop and two shorter helices (H5 and H6), closer to the C terminus, forming a helix-turn-helix motif. A large extramembrane domain encompasses β-strands (S1–S6) and α-helices (H3 and H4). A remarkable feature of this domain (EM2) is the extended hairpin formed by the S1–S2 strands, whose tip is most of the time interacting with the membrane leaflet. MD simulations showed stability of the whole TMD, whereas the EM2 domain displayed higher fluctuations due to occasional loss of the interaction with the membrane.

The orientation of TMEM151A extramembrane domains has been defined by two different wet experimental approaches such as live-IF and electron microscopy. Indeed, surface labeling showed that the HA epitope in the loop among the H1 and H2 helices (TMEM151A-HA-LOOP) is facing outwards from the plasma membrane validating the predicted topology. In addition, electron microscopy images confirm its localization on the extracellular side of the plasma membrane as well as in the inner side of the intracellular vesicles. On the contrary the HA epitope at the C-term (TMEM151A-HA) is associated to the cytosolic face of the plasma membrane, ER or endosome membranes. Taken together these results indicate that TMEM151A has a short extracellular loop, a structured and stable transmembrane domain and a large cytosolic domain featuring several secondary structures, suggesting the involvement of TMEM151A in processes occurring in the cytosol or at the membrane level but not extracellularly.

In addition to TMEM151A, the only other gene associated with PKD, with higher frequency, is PRRT2, a transmembrane protein with a similar expression pattern in the central nervous system.[14,17]

From the topological point of view PRRT2 is characterized by an unstructured cytosolic domain and a particular membrane associated domain with a helix-hinge-helix not crossing the plasma membrane contiguous to a single transmembrane helix, that is a hallmark of several Dispanins, the class to which PRRT2 belongs.[21,43,44] This particular structure is a feature of proteins involved in intracellular (or vesicles) trafficking and membrane fusion events. Interestingly, a similar domain is also present in the TMD of TMEM151A, providing insights into its putative function. However, the helix-hinge-helix motif of TMEM151A is adjacent to transmembrane helices in 3D structure but not contiguous to them in the protein sequence. On the contrary, the intracellular domain of TMEM151A is very different from the unstructured cytosolic domain of PRRT2 suggesting that the two proteins may share some functions at the membrane level but are involved in different processes in the cytosol.

Our results provide preliminary hints regarding the subcellular expression of TMEM151A. Due to the lack of commercially available antibodies recognizing, by immunofluorescence assay, the endogenous protein, the only knowledge we have about the subcellular localization of TMEM151A comes from overexpression studies in cell culture performed by Li et al.[1] in which the protein localizes mostly at the ER. They likely did not observe any signal at the plasma membrane because the staining was performed exclusively under permeabilized conditions. Our data from IF and electron microscopy of the TMEM151A overexpressed constructs demonstrated that its expression is not just restricted to internal membranes such as ER, but it extends also to the plasma membrane. These results suggest the involvement of TMEM151A, albeit within the limitations of these overexpression assays, in intracellular trafficking processes that also involve the plasma membrane. To confirm these results on the endogenous protein, further studies on its expression and localization are nec-

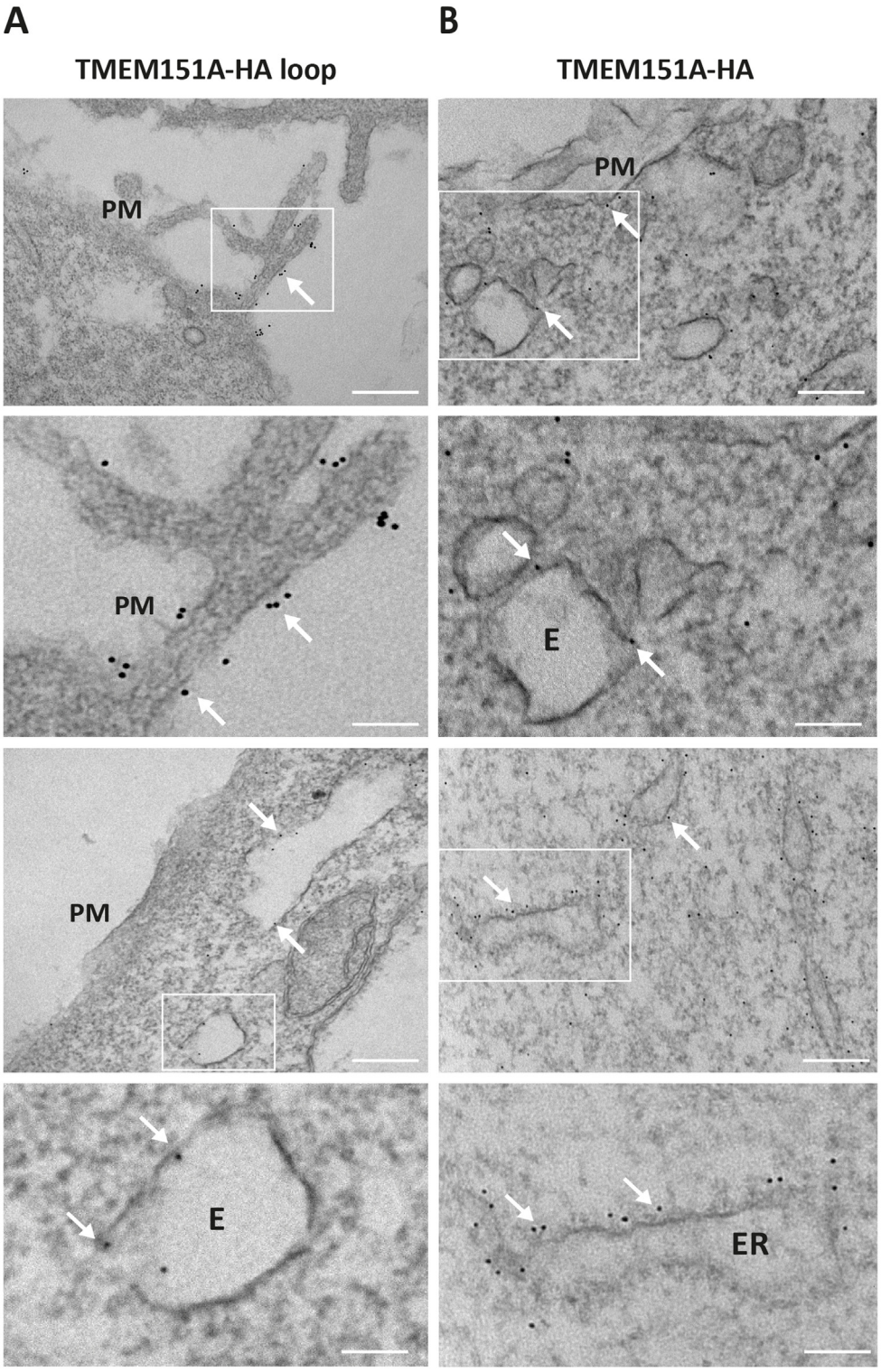

Figure 5. Electron microscopy confirms the predicted topology of TMEM151A. A. Electron micrographs show the localization of the TMEM151A-HA loop with gold particles on the outer side of plasma membrane protrusions (upper image, white box indicates zoomed detail) and on the inner side of a putative endosomal structure (lower image, white box indicates zoomed detail). B. Electron micrographs depict the localization of TMEM151A-HA with gold particles on the inner side of the plasma membrane and on the outer side of endosomal structures (upper image) and endoplasmic reticulum (lower image). White boxes indicate zoomed-in details. PM: plasma membrane; E: putative endosome; ER: endoplasmic reticulum. White arrows indicate gold particles. Scale bars: 200 nm; 100 nm for insets.

essary. In particular, it will be important to assess whether TMEM151A is located also in specific neuronal subcompartments such as the axon, presynaptic terminals or postsynaptic zones.

From our topology data it can be concluded that TMEM151A plays its role in the membrane of intracellular organelles and in the plasma membrane as well as in the cytosolic cellular compartment. Future interactomics studies addressing the identification of possible molecular partners could clarify the specific pathways in which TMEM151A is involved as well as the underlying mechanisms of paroxysmal disorders caused by its mutations. Overall, this work may contribute in directing the future research to specific groups of molecular interactors and molecular targets for pharmacological interventions.

CRediT authorship contribution statement

Lisastella Morinelli: Writing – original draft, Visualization, Methodology, Investigation, Formal analysis, Data curation. **Beatrice Corradi:** Writing – original draft, Formal analysis, Data curation. **Pietro Arnaldi:** Investigation. **Katia Cortese:** Methodology, Formal analysis. **Martina Muià:** Validation. **Federico Zara:** Funding acquisition. **Luca Maragliano:** Writing – review & editing, Formal analysis. **Bruno Sterlini:** Writing – review & editing, Writing – original draft, Supervision, Formal analysis, Conceptualization. **Anna Corradi:** Writing – review & editing, Writing – original draft, Supervision, Project administration, Methodology, Funding acquisition, Conceptualization.

DATA AVAILABILITY

Data will be made available on request.

DECLARATION OF COMPETING INTEREST

The authors declare that they have no known competing financial interests or personal relationships that could have appeared to influence the work reported in this paper.

Acknowledgement

All the cartoons were created using Biorender.com.

We are grateful to Dr. Maria Cristina Gagliani for her help in electron microscopy experiments and to Dr. Silvia Casagrande and Dr. Antonella Marte for cell culture experiments.

We also gratefully acknowledge the Data Science and Computation Facility and its Support Team at Fondazione Istituto Italiano di Tecnologia.

Consent for publication

All authors have read and approved this publication.

Funding

The study was supported by Telethon/Cariplo Foundations – Italy (Grant GJC22066 to AC and FZ), by IRCCS Ospedale Policlinico San Martino Genova (Ricerca Corrente and "5X1000"_to AC), by #NEXTGENERATIONEU (NGEU) and funded by the Ministry of University and Research (MUR), National Recovery and Resilience Plan (NRRP), project MNESYS (PE0000006) – A Multiscale integrated approach to the study of the nervous system in health and disease (DN. 1553 11.10.2022). The University of Genoa funded the acquisition of the HITACHI 120 kV TEM microscope HT7800, (Grant D.R. 3404, 2018, Grandi Attrezzature/Heavy Equipment)".

Appendix A. Supplementary material

Supplementary material to this article can be found online at https://doi.org/10.1016/j.jmb.2024.168834.

Received 9 August 2024;
Accepted 20 October 2024;
Available online 23 October 2024

Keywords:
protein topology;
paroxysmal kinesigenic dyskinesia;
transmembrane protein;
TMEM151A;
molecular dynamics simulation

† Authors equally contributed to this work and share first authorship.

References

1. Li, H.-F. et al, (2021). TMEM151A variants cause paroxysmal kinesigenic dyskinesia. *Cell Discov.* **7** https://doi.org/10.1038/s41421-021-00322-w.
2. Li, Y.-L. et al, (2022). Exome-wide analyses in paroxysmal kinesigenic dyskinesia Confirm TMEM151A as a novel causative gene. *Mov. Disord.* **37** (3), 641–643. https://doi.org/10.1002/mds.28904.
3. Tian, W.-T. et al, (2022). TMEM151A variants cause paroxysmal kinesigenic dyskinesia: A large-sample study. *Mov. Disord.* **37** (3), 545–552. https://doi.org/10.1002/mds.28865.

4. Wang, H., Huang, P., Zhu, M., Fang, X., Wu, C., Hong, D., (2022). TMEM151A phenotypic spectrum includes paroxysmal kinesigenic dyskinesia with infantile convulsions. *Neurol. Sci.* **43** (10), 6095–6099. https://doi.org/10.1007/s10072-022-06208-3.
5. Wirth, T. et al, (2022). De Novo mutation in TMEM151A and paroxysmal kinesigenic dyskinesia. *Mov. Disord.* **37** (5), 1115–1117. https://doi.org/10.1002/mds.29023.
6. Ma, L.-Y., Han, L., Niu, M., Chen, L., Yu, Y.-Z., Feng, T., (2023). Screening of the TMEM151A gene in patients with paroxysmal kinesigenic dyskinesia and other movement disorders. *Front. Neurol.* **13**, 2022. https://doi.org/10.3389/fneur.2022.865690.
7. Chen, Y.-L., Chen, D.-F., Li, H.-F., Wu, Z.-Y., (2022). Features differ between paroxysmal kinesigenic dyskinesia patients with PRRT2 and TMEM151A variants. *Mov. Disord. Off. J. Mov. Disord. Soc.* **37** (3), 608–613. https://doi.org/10.1002/mds.28939.
8. Satolli, S. et al, (2023). Two cases of TMEM151A-associated paroxysmal dyskinesia in a single-center series of PRRT2-negative patients. *Mov. Disord. Clin. Pract.* **10** (5), 842–844. https://doi.org/10.1002/mdc3.13705.
9. Huang, H.L. et al, (2023). TMEM151A variants associated with paroxysmal kinesigenic dyskinesia. *Hum. Genet.* **142** (8), 1017–1028. https://doi.org/10.1007/s00439-023-02535-3.
10. Zhang, Y. et al, (2024). Genetic and phenotypic analyses of PRRT2 positive and negative paroxysmal kinesigenic dyskinesia. *Ther. Adv. Neurol. Disord.* **17** https://doi.org/10.1177/17562864231224110.
11. Xu, J.-J., Li, H.-F., Wu, Z.-Y., (2024). Paroxysmal kinesigenic dyskinesia: genetics and pathophysiological mechanisms. *Neurosci. Bull.* **40** (7), 952–962. https://doi.org/10.1007/s12264-023-01157-z.
12. Ebrahimi-Fakhari, D., Saffari, A., Westenberger, A., Klein, C., (2015). The evolving spectrum of PRRT2-associated paroxysmal diseases. *Brain* **138** (12), 3476–3495. https://doi.org/10.1093/brain/awv317.
13. Landolfi, A., Barone, P., Erro, R., (2021). The spectrum of PRRT2-associated disorders: update on clinical features and pathophysiology. *Front. Neurol.* **12** https://doi.org/10.3389/fneur.2021.629747.
14. Fruscione, F. et al, (2018). PRRT2 controls neuronal excitability by negatively modulating Na+ channel 1.2/1.6 activity. *Brain* **141** (4), 1000–1016. https://doi.org/10.1093/brain/awy051.
15. Franchi, F. et al, (2023). The intramembrane COOH-terminal domain of PRRT2 regulates voltage-dependent Na^+ channels. *J. Biol. Chem.* **299**, (5) https://doi.org/10.1016/j.jbc.2023.104632 104632.
16. Sterlini, B. et al, (2023). Missense mutations in the membrane domain of PRRT2 affect its interaction with Nav1.2 voltage-gated sodium channels. *Neurobiol. Dis.* **183**, https://doi.org/10.1016/j.nbd.2023.106177 106177.
17. Valente, P. et al, (2016). PRRT2 is a key component of the Ca^{2+}-dependent neurotransmitter release machinery. *Cell Rep.* **15** (1), 117–131. https://doi.org/10.1016/j.celrep.2016.03.005.
18. Sterlini, B. et al, (2021). An interaction between PRRT2 and Na+/K+ ATPase contributes to the control of neuronal excitability. *Cell Death Dis.* **12**, (4) https://doi.org/10.1038/s41419-021-03569-z 4.
19. Michetti, C., Corradi, A., Benfenati, F., (2017). PRRT2, a network stability gene. *Oncotarget* **8** (34), 55770–55771. https://doi.org/10.18632/oncotarget.19506.
20. Marx, S. et al, (2020). Transmembrane (TMEM) protein family members: Poorly characterized even if essential for the metastatic process. *Semin. Cancer Biol.* **60**, 96–106. https://doi.org/10.1016/j.semcancer.2019.08.018.
21. Rossi, P. et al, (2016). A novel topology of proline-rich transmembrane protein 2 (PRRT2): Hints for an intracellular function at the synapse*. *J. Biol. Chem.* **291** (12), 6111–6123. https://doi.org/10.1074/jbc.M115.683888.
22. Ferrante, D. et al, (2021). PRRT2 modulates presynaptic Ca^{2+} influx by interacting with P/Q-type channels. *Cell Rep.* **35**, (11) https://doi.org/10.1016/j.celrep.2021.109248 109248.
23. Jumper, J. et al, (2021). Highly accurate protein structure prediction with AlphaFold. *Nature* **596**, (7873) https://doi.org/10.1038/s41586-021-03819-2 7873.
24. Lomize, M.A., Pogozheva, I.D., Joo, H., Mosberg, H.I., Lomize, A.L., (2012). OPM database and PPM web server: resources for positioning of proteins in membranes. *Nucleic Acids Res.* **40** (D1), D370–D376. https://doi.org/10.1093/nar/gkr703.
25. The PyMOL Molecular Graphics System, Version 2.0. (2002). Schrödinger, LLC, New York, NY.
26. Lee, J. et al, (2019). CHARMM-GUI membrane builder for complex biological membrane simulations with glycolipids and lipoglycans. *J. Chem. Theory Comput.* **15** (1), 775–786. https://doi.org/10.1021/acs.jctc.8b01066.
27. Neria, E., Fischer, S., Karplus, M., (1996). Simulation of activation free energies in molecular systems. *J. Chem. Phys.* **105** (5), 1902–1921. https://doi.org/10.1063/1.472061.
28. Lee, J. et al, (2016). CHARMM-GUI input generator for NAMD, GROMACS, AMBER, OpenMM, and CHARMM/OpenMM simulations using the CHARMM36 additive force field. *J. Chem. Theory Comput.* **12** (1), 405–413. https://doi.org/10.1021/acs.jctc.5b00935.
29. Best, R.B. et al, (2012). Optimization of the additive CHARMM all-atom protein force field targeting improved sampling of the backbone φ, ψ and side-chain $\chi(1)$ and $\chi(2)$ dihedral angles. *J. Chem. Theory Comput.* **8** (9), 3257–3273. https://doi.org/10.1021/ct300400x.
30. Huang, J. et al, (2017). CHARMM36: An improved force field for folded and intrinsically disordered proteins. *Biophys. J.* **112** (3), 175a–176a. https://doi.org/10.1016/j.bpj.2016.11.971. Supplement 1.
31. Darden, T., York, D., Pedersen, L., (1993). Particle mesh Ewald: An Nṡlog(N) method for Ewald sums in large systems. *J. Chem. Phys.* **98** (12), 10089–10092. https://doi.org/10.1063/1.464397.
32. Miyamoto, S., Kollman, P.A., (1992). Settle: An analytical version of the SHAKE and RATTLE algorithm for rigid water models. *J. Comput. Chem.* **13** (8), 952–962. https://doi.org/10.1002/jcc.540130805.
33. Feller, S.E., Zhang, Y., Pastor, R.W., Brooks, B.R., (1995). Constant pressure molecular dynamics simulation: The Langevin piston method. *J. Chem. Phys.* **103** (11), 4613–4621. https://doi.org/10.1063/1.470648.
34. Humphrey, W., Dalke, A., Schulten, K., (1996). VMD: Visual molecular dynamics. *J. Mol. Graph.* **14** (1), 33–38. https://doi.org/10.1016/0263-7855(96)00018-5.

35. Kožić, M., Bertoša, B., (2024). Trajectory maps: molecular dynamics visualization and analysis. *NAR Genom. Bioinfor.* **6**, (1) https://doi.org/10.1093/nargab/lqad114 lqad114.
36. Abramson, J. et al, (2024). Accurate structure prediction of biomolecular interactions with AlphaFold 3. *Nature* **630** (8016), 493–500. https://doi.org/10.1038/s41586-024-07487-w.
37. Altschul, S.F., Gish, W., Miller, W., Myers, E.W., Lipman, D.J., (1990). Basic local alignment search tool. *J. Mol. Biol.* **215** (3), 403–410. https://doi.org/10.1016/S0022-2836(05)80360-2.
38. Wallace, I.M., O'Sullivan, O., Higgins, D.G., Notredame, C., (2006). M-Coffee: combining multiple sequence alignment methods with T-Coffee. *Nucleic Acids Res.* **34** (6), 1692–1699. https://doi.org/10.1093/nar/gkl091.
39. Moretti, S., Armougom, F., Wallace, I.M., Higgins, D.G., Jongeneel, C.V., Notredame, C., (2007). The M-Coffee web server: a meta-method for computing multiple sequence alignments by combining alternative alignment methods. *Nucleic Acids Res.* **35** (Web Server issue), W645–W648. https://doi.org/10.1093/nar/gkm333.
40. Robert, X., Gouet, P., (2014). Deciphering key features in protein structures with the new ENDscript server. *Nucleic Acids Res.* **42** (Web Server issue), W320–W324. https://doi.org/10.1093/nar/gku316.
41. Mattingly, R.R., Macara, I.G., (1996). Phosphorylation-dependent activation of the Ras-GRF/CDC25Mm exchange factor by muscarinic receptors and G-protein beta gamma subunits. *Nature* **382** (6588), 268–272. https://doi.org/10.1038/382268a0.
42. Polishchuk, E.V., Polishchuk, R.S., (2019). Pre-embedding labeling for subcellular detection of molecules with electron microscopy. *Tissue Cell* **57**, 103–110. https://doi.org/10.1016/j.tice.2018.11.002.
43. Almén, M.S., Bringeland, N., Fredriksson, R., Schiöth, H. B., (2012). The dispanins: A novel gene family of ancient origin that contains 14 human members. *PLOS ONE* **7** (2), e31961. https://doi.org/10.1371/journal.pone.0031961.
44. Deuis, J.R., Klasfauseweh, T., Walker, L., Vetter, I., (2024). The 'dispanins' and related proteins in physiology and neurological disease. *Trends Neurosci.*. https://doi.org/10.1016/j.tins.2024.06.004.